GRASS GIS Modules for Topographic and Geophysical Analysis of the ETOPO1 DEM and Raster Data: North Fiji Basin, Pacific Ocean

Polina Lemenkova

GRASS GIS MODULES FOR TOPOGRAPHIC AND GEOPHYSICAL ANALYSIS OF THE ETOPO1 DEM AND RASTER DATA: NORTH FIJI BASIN, PACIFIC OCEAN

Polina Lemenkova[1]

Abstract: - GRASS GIS Modules for Topographic and Geophysical Analysis of the ETOPO1 DEM and Raster Data: North Fiji Basin, Pacific Ocean *The paper presents topographic analysis based on the raster data (NetCDF and grid formats) and visualization of the geophysical datasets that resembles the topographic surface. Geographically, the research focuses on the region of North Fiji Basin, South Pacific Ocean. North Fiji Basin is one of the marginal basins located at the converging boundary between the Pacific and Australian tectonic plates and is notable for complex geological settings. Methodology is based on GRASS GIS and includes scripting and cartographic visualization. Data include ETOPO1, GEBCO, EGM96 gravity and geoid raster grids imported to GRASS GIS via GDAL library ('r.in.gdal' module) from NetCDF and GRD formats, evaluated and visualized. Several GRASS modules were used as a sequential scripting for displaying and modelling data. Geomorphometric analysis (slopes, curvature, aspect, elevation) was performed by module 'r.slope.aspect' based on ETOPO1 grid. Statistical data analysis (histograms, polar diagram) for topographic and geoid gravitational fields were visualized by combination of GRASS modules d.rast, g.region, d.polar, d.histogram, d.grid, d.legend, d.text. Topographic analysis reveal that free-air gravity anomaly mark the continental shelf-slope border showing that generally, geophysical settings are dominated by the topographic effect. These observations are consistent with the inferred prominent role of the geophysical settings. The histograms reveal that topography (trenches, abyssal plains, shelf areas) has values between -5,000 and -1,000 m, and a clear peak with major values between 100 and 350 m above sea level. This distribution indicates that dominating depths of the ocean floor in North Fiji Basin are between -1,500 to -3,000 m. The aspect map of the ETOPO1 initial raw raster grid show that the surface has mostly 50°-110° oriented slope followed by data range in 250°-300° oriented slopes which is well correlating with submarine topography and general relief forms. The steepening of the gravity values between 50 and 55 mGal and 58 to 63 mGal indicates geoid undulations suggesting that bathymetry is controlled by the geological settings in the study area. Console-based scripts of GRASS GIS are presented together with cartographic outputs showing its effectiveness for the geographic spatial analysis.*

Keywords: GRASS GIS, transect, profile, topography, Fiji, Pacific Ocean, bathymetry

1. Introduction

Study area is located in the North Fiji Basin, south-west Pacific Ocean. The North Fiji Basin is one of the marginal basins located at the converging boundary between the Pacific and Australian tectonic plates (*Auzende et al. 1986*). It lies between the New Hebrides arc-trench system to the west, the Fiji Platform to the east, the Vityaz Trench subduction zone to the north, and the arcuate Matthew-Hunter zone to the south, Fig. 1.

1.1. Topographic settings

An elevated relief is characteristic for the South Fiji Basin (*Davey, 1982)*. The surface of its seafloor bottom is slightly tilted to the north with depths ranging from 4000 to 4500 m. Depths of 2500–3000 m prevail on the North Fijian plateau (North Fiji Basin), depths of lesser than 2500 m predominate to the east of the Fiji islands in Lau Basin where back-arc lavas are recorded (*Keller et al., 2007*). The surface relief of the plateau is hilly and ridged with some separate higher seamounts and narrow small hollows. The ridge

1 Schmidt Institute of Physics of the Earth, Russian Academy of Sciences. Laboratory of Regional Geophysics and Natural Disasters (Nr. 303). Bolshaya Gruzinskaya St, 10, Bld. 1, Moscow, 123995, Russian Federation. ORCID ID: 0000-0002-5759-1089. Tel.: +7-916-298-37-19. Email: pauline.lemenkova@gmail.com.

of the islands of Santa Cruz and New Hebrides, is located along the western edge of the plateau, north to the Vanuatu Trench (Fisher et al., 1963; *Collot et al., 1985*). Hunter Ridge located on the south of North Fiji Basin is notable for the small islands and reefs (*Ishibashi et al., 1994*).

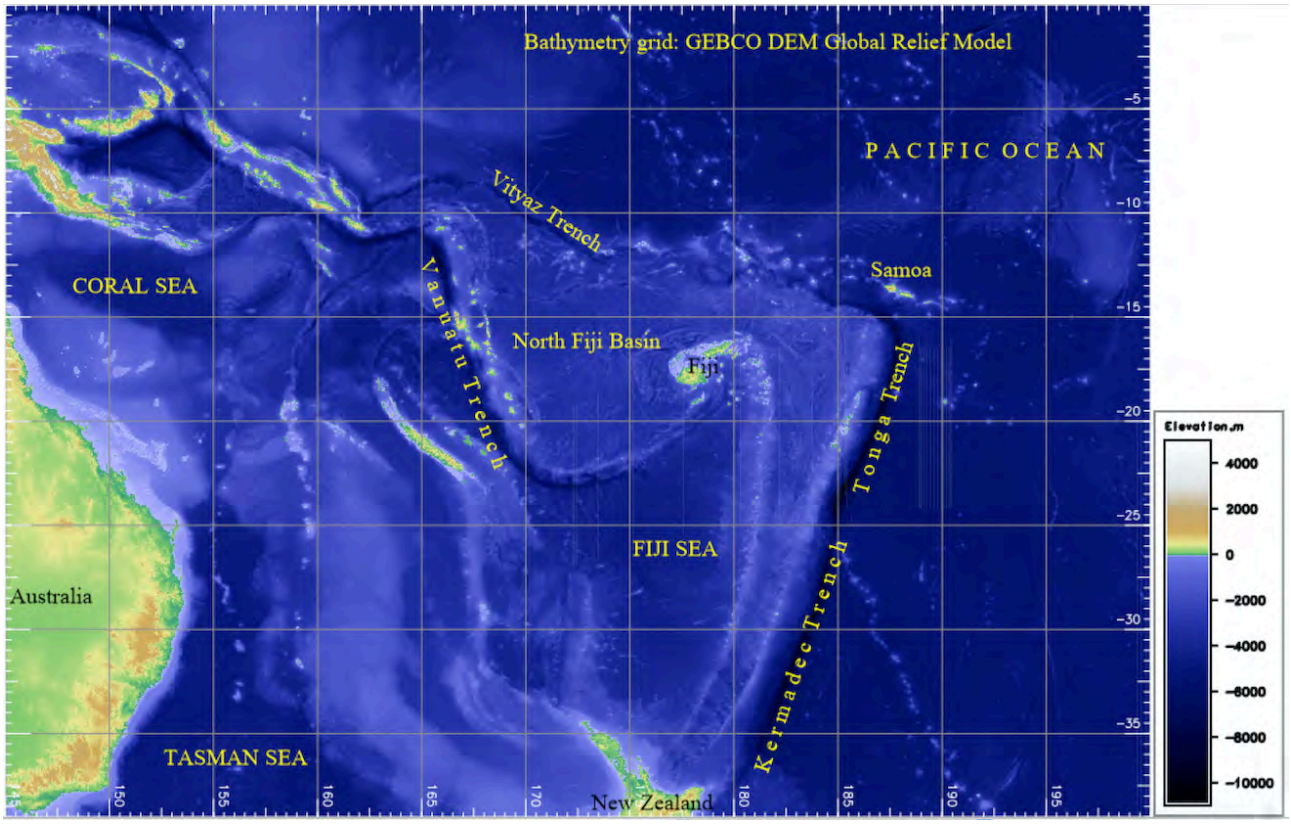

Fig. 1. Bathymetry map of the study area. Raster based on GEBCO 15 arc-second global relief model of Earth's surface, Fiji region, south Pacific Ocean. Visualization of the grid (.grd) file extracted as a subset of NetCDF file (vt_relief.nc) in geographic format, color table=srtm_plus. Mapping: GRASS GIS.
Source: author.

Northern border of the North Fiji Basin is marked by the Vityaz Trench with a maximum depth of 6150 m. In the southeastern part of the North Fiji Basin there is a vast elevated hill on with volcanic Fiji islands and numerous coral reefs are located. A double ridge stretches from the eastern edge of the North Fiji Basin towards the New Zealand. Western part of this ridge is represented by the Lau-Colville Ridge in the Lau Basin (Hahm et al., 2012), a remnant arc stretching on the western and eastern sides of the basin (Gill, 1976). Eastern part is represented by the Tonga ridge and parallel trench with volcanic islands where it has recently been detected that Pacific Plate crust is 5.5 km thick with a velocity structure similar to the East Pacific Rise (*Crawford et al. 2003)*.

1.2. Geologic settings

South Fiji Basin has a structure of the crust close to the oceanic type. The thickness of such crust is 7–11 km, the consolidated layers are characterized by the seismic wave velocities of 4.4–6.0 and 6.8–7.0 km/s. A mantle is located beneath oceanic crust with boundary velocities of 8.1–8.4 km/s.

North Fiji Basin does not exceed 10 km with velocities in the consolidated layers 3.3–5.5 and 6.4–6.6 km/s in the thickness of its crust. However, below the oceanic crust of Fiji region is located zone of the anomalous mantle with lower velocities (7.3–7.7 km/sec), which, according to gravimetric data, extends to depths of ca. 25 km (Litvin, 1987).

Tonga and Kermadec trenches are stretching parallel to the island arcs according

to the formation processes well described in the literature (*Hess, 1962; Hawkins et al. 1984;* Kious and Tilling, 1996). Tonga–Kermadec island arc and parallel Collvil-Lau ridge are characterized by a subcontinental type of crust with a thickness of 14–18 km. The layers below the thin volcanic-sedimentary layer have seismic velocity speeds at 5.1–6.2 and 6.5–7.0 km/sec (*Dubois et al., 1973)*. The bottom of the deep-sea trenches is characterized by the thickness of the crust <10 km with seismic velocities 5.2-5.5 to 6.5-7.0 km/sec (Litvin, 1987). Further geological investigation on Fiji Basin are presented in literature (*Bendel, 1993; Boespflug, 1990; Daniel, 1982; Maillet et al., 1989; Gracia-Mont, E., 1991*).

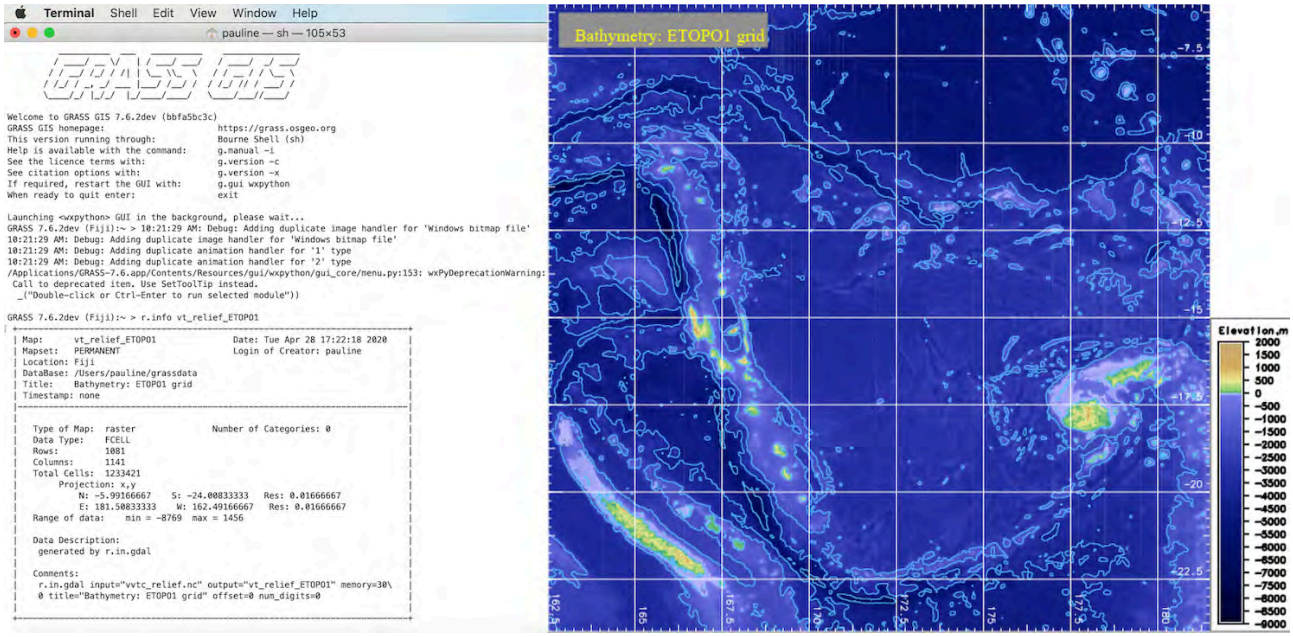

Fig. 2. Enlarged bathymetry map of the Fiji region: ETOPO1 raster, 1 arc-minute global relief model of Earth's surface. Left: GRASS GIS shell scripting console. Right: GRASS GIS map output. Source: author.

1.3. Geophysical settings

The most part of the North Fiji Basin is notable for sub-latitudinal magnetic anomalies with an intensity of 200 to 700 gammas, which are correlated with a dissected hilly ridge relief (*Maillet et al., 1986*). In the eastern part of the North Fiji Basin, the direction of the magnetic anomalies changes to the sub-meridional, which continues along the Lau-Colville Ridge, the Tonga–Kermadec island arc and in the hollow in between them (*Auzende et al., 1995)*. Such differences in the anomalies may indicate that there is a local zone of the spreading of the ocean seafloor marked by linear magnetic anomalies (*Taylor et al., 1996*). The magnetic field becomes relatively calm above the Tonga and Kermadek trenches without any significant anomalies.

Transition zones eastward of New Guinea and Australia are characterized by the well-defined linear directions of the high and low Faye anomalies, which in general reflects the geometry of the forms of the submarine relief. Slightly higher values of Faye anomalies are noted in the northern part of the region compared with the southern one. For example, New Guinea Sea and the northern part of the Coral Sea has mostly positive Faye anomalies (50–70 mGal), while Fiji and Tasman seas – slightly negative ones.

Elongated zones of intense positive Faye anomalies (100-170 mGal) are traced over the submarine ridges of Lord Howe Rise (Lord Howe Seamount Chain), Norfolk Ridge, Lau-Colville Ridge, and over the island arc of Tonga-Kermadec (Litvin, 1987). Tonga and Kermadec trenches are characterized by a large negative Faye anomaly (up to -210 mGal). The Bouguer anomalies are positive almost everywhere in the region as follows: 40 to 60 above the submarine ridges, 160 to 240 above the island arcs with volcanic structures, 240 to 320 mGal

in the basins, and >400 along the Tonga and Kermadec trenches (*Gaynanov, 1980*). The marine free-air gravity anomalies are shown on the map visualized on Fig. 4 (right) with information on the data, Fig. 4 (left).

2. Methods

Methods is based on using GRASS GIS version 7.6 (Neteler, 2000; Neteler and Mitasova, 2008) with specific application of module r.profile for topographic analysis through plotting cross-sectional profiles. Methodology of this paper aims to visualize and model topographic surface maps in the study area of Fiji area and assess the applicability and effectiveness of GRASS GIS for cartographic data processing. In order to do so several grids (ETOPO1, gravity and geoid datasets) have been imported to GRASS GIS using GDAL library via 'r.in.gdal' module, comparatively evaluated (data range and extension) and visualized.

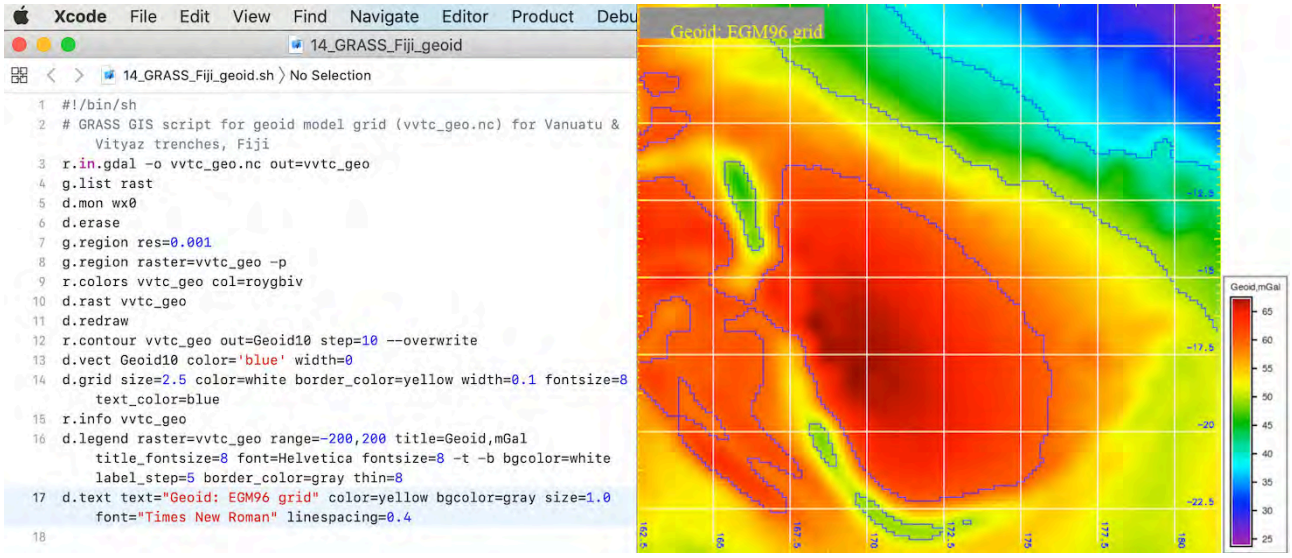

Fig. 3. Geoid model based on the Earth Gravitational Model EGM96, Fiji region, south Pacific Ocean. Left: GRASS GIS shell script in Xcode environment. Right: GRASS GIS map. GRASS GIS. Source: author.

Technically, importing, displaying and computing DEMs was performed by several GRASS modules as a sequential use: 'r.in.gdal' for data import, 'd.mon' and 'd.rast' for visualization of raster data on a GRASS display. The g.region module was used to manage the settings of the current geographic region (162.5° 181.5° E, 24° to 6.0° S). These regional boundaries were set directly in GRASS command line. Module 'r.colors' was used to modify and select color tables for raster maps. Plotting isolines was done using modules 'r.contour' and 'd.vect', whereby r.contour was applied to generate a set of topographic contours from raster maps, followed by d.grid for their visualization, respectively. The 'd.legend' and 'd.text' modules were used for annotating maps and visualizing color legends for each of the maps. As as result elevation data and gravity fields were represented by raster maps with digitized contours read from the or measured points in ASCII format. Visualization of the grid (.grd) file was extracted as a subset of NetCDF file (vvtc_relief.nc) in geographic format, color table=srtm_plus [Fig. 2].

Topographic (or geomorphometric) analysis was performed by GRASS provides tool 'r.slope. aspect' via the following code: 'elevation=vt_ relief_ETOPO1 slope=slope aspect=aspect pcurvature=pcurv tcurvature=tcurv'. As a result, a set of geomorphometric parameters representing geometrical properties of the land surface (slope, profile curvature, aspect, tangential curvature and elevations) was computed. Calculated from DEM both at cell points and in their immediate surroundings, geomorphometric parameters describe local land-surface properties on the oceanic seafloor and indicate slope steepness and geographic disposition of the aspect (north,

south, west, east). The geomorphometry [Fig. 6 and 7] and statistical data distribution for topographic and geoid gravitational fields [Fig. 8] were visualized using GRASS modules d.rast, d.polar, d.histogram, as well as auxiliary modules (d.grid, d.legend, d.text). Geomorphometric analysis [Fig. 6 and 7] of the local parameters (slope, aspect, curvatures and derivatives) was based on the principles of differential geometry of the topographic slopes derived from DEMs (ETOPO1 raster grid) using partial derivatives of the mathematical function representing the surface from the embedded functions of GRASS GIS. Polar diagram was displayed [Fig. 6, right] to show distributions of slope aspect values by the 'd.polar' GRASS module.

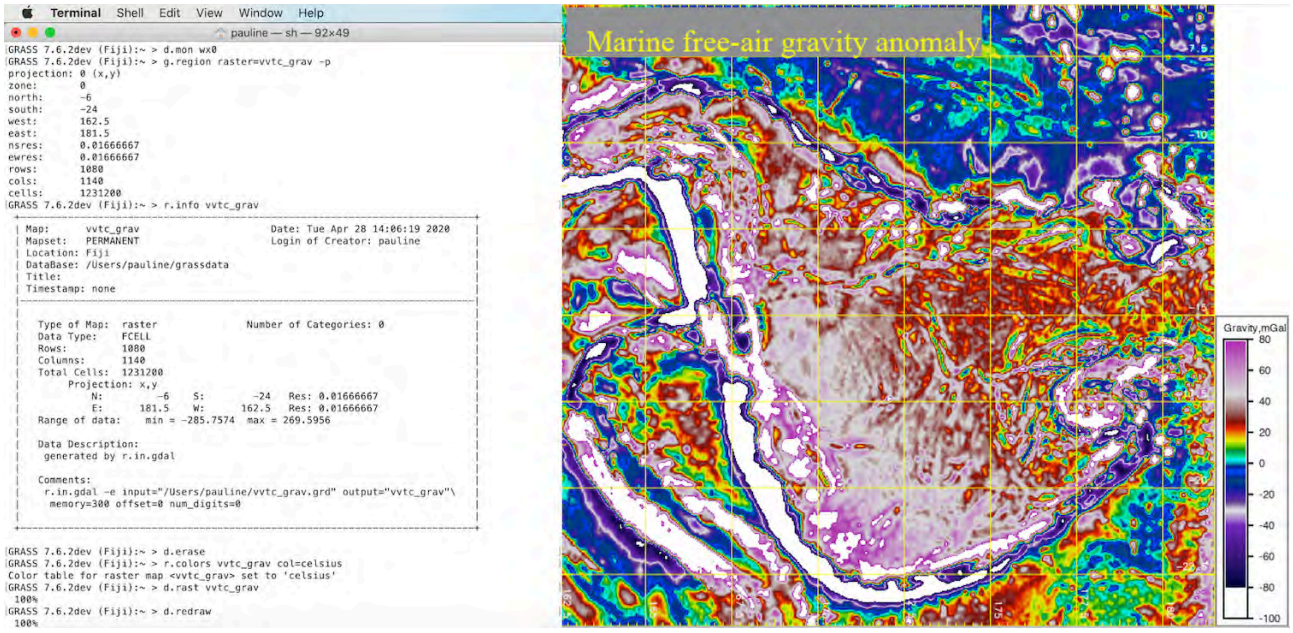

Fig. 4. GRASS GIS scripting in console menu for mapping marine free-air gravity anomaly, Fiji region, south Pacific Ocean. Left: GRASS GIS shell console. Right: GRASS GIS map output. Source: author.

The results of topographic mapping and gravimetric modeling are presented using GRASS GIS modules. Several GRASS modules (r.countour, d.vect, d.rast, d.grid, d.legend, d.text, etc.) were applied and tested in this work in order to decide on their applicability on raster data processing and technical functionality of GRASS GIS. The geoid model [Fig. 3] was made using 1-mGal accuracy, corrected marine free-air gravity anomaly grid derived from the Geosat and ERS-1 satellite altimetry (Andersen et al., 2009; Sandwell & Smith, 2009) for the Fiji region, 162.5° to 181.5°E, 24°to 6°S. The visualization of the grid (.grd) file extracted as a subset of NetCDF file (vvtc_geo.nc) in geographic format was based on EGM96 raster. The grids were compiled from existing terrestrial, marine and satellite free-air altimetry-derived gravity data. Data of gravity grids were taken from the repositories of the Satellite Geodesy research group at Scripps Institution of Oceanography, University of California (Smith and Sandwell, 1995) based on the latest global gravity model from CryoSat-2 and Jason-1 altimeter satellites and depth soundings at 15 arc second resolution (Wingham et al., 2006).

Marine vertical free-air gravity anomaly map of North Fiji Basin area and its surroundings [Fig. 5] has been compiled using previously published open access data (Sandwell & Smith, 2005; 2009; Garcia et al., 2013). The dataset includes gravity data in high resolution covering the North Fiji and Lau basins, southern Pacific Ocean. High free-air gravity anomaly mark the continental shelf-slope border showing that generally, it is dominated by the topographic effect. Fig. 4 showing marine free-air gravity anomaly of the study area has been plotted through visualization of the grid (.grd) file extracted as a subset of img file (grav_27.1.img) in geographic

format based on CryoSat-2 measurements. The free air gravity anomaly is a standard for oceanic gravity interpretation. Marine free-air gravity has been corrected for the gravity effect caused by the elevation difference between the location of a station where gravity measurements took place, and a sea level (distance).

Practical value of the gravity mapping consists in the indirect way to visualize different physical properties and density of the ocean seafloor rocks by remote sensing. Since various rock types contrast in density, this causes gravity anomalies. For instance, sedimentary rocks usually have low densities and are characterized by gravity lows on the marine free-air gravity anomaly maps. On the contrary, rocks containing high-density minerals are associated with gravity highs. Hence, marine free-air gravity maps can practically assist in identification of the geological studies indicating underlying rocks on the seafloor, geologic fault lines, geological exploration (mineral resources, deposits), and reservoirs.

Free-air gravity anomaly [Fig. 5] is based on the available raster created by open source datasets from the altimeter data (EGM96). Heavy contour interval is given at 10 mGal. Topographic analysis and modelling applications on slope, aspect, curvature and elevations require calculation of DEM cells and estimation of some geomorphological parameters. GRASS GIS module 'r.slope.aspect' with flags on input/output raster grids, and other parameters enables to visualize these maps [Fig. 6 and 7]. Method of polar diagram plotting was developed by Hofierka et al. (2009) and used in GRASS by 'd.polar' module for drawing polar diagram of angle aspect map of the Fiji Basin.

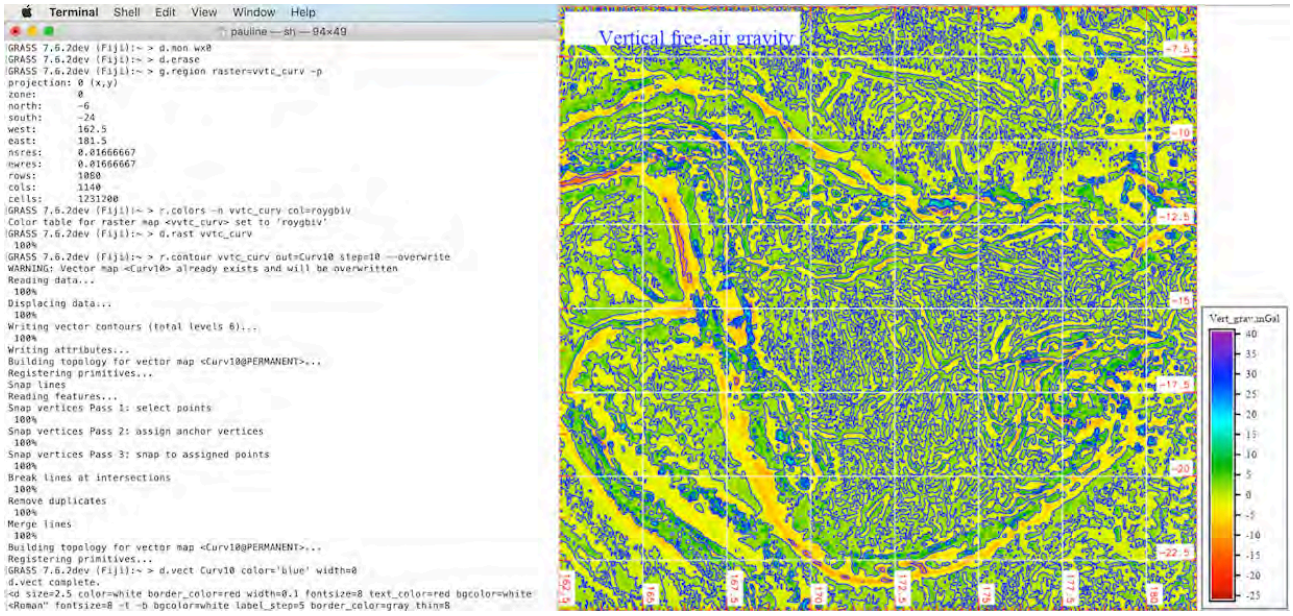

Fig. 5. Vertical marine free-air gravity anomaly, Fiji region, south Pacific Ocean. Visualization of the grid (.grd) file extracted as a subset of img file (vvtc_curv.grd) in geographic format based on CryoSat-2 measurements. Left: GRASS GIS shell console. Right: GRASS GIS map output. Source: author.

3. Results and Discussion

The assessment of the results is based on topographic mapping of the region covering North Fiji Basin, southern Pacific Ocean. The presented maps are comparatively applied on the study area and thematic settings compared (topography, gravity, slope aspect and curvature), in order to evaluate the correlation in the bathymetry related to the geophysical processes. The aspect map [Fig. 6, left] for the region of North Fiji Basin is based on recalculated ETOPO1 DEM with a resolution of 1 min and derived from the contours plotted with every 2000 isobath [Fig. 2]. Calculated slope of the initial topographic grid shows peaks in the polar diagram [Fig. 6 right] indicating a NE-SW elongated ellipse in topographic orientation. The aspect map of the

ETOPO1 initial raw raster grid show that the majority of the surface has 50°-110° oriented slope (Fig. 6, left, bright green colors). Other notable data range is representing 250° to 300° oriented slopes (Fig. 6, left, reddish colors) well correlating with submarine topography [Fig. 2] and general relief forms.

A set of topographic raster maps (aspect, profile curvature, tangential curvature, slope) was computed automatically by GRASS with ETOPO1 DEM interpolation from the isolines: 'r.slope.aspect elevation=vt_relief_ETOPO1 slope=slope aspect=aspect pcurvature=pcurv tcurvature=tcurv'. The polar diagram (Fig. 6, right) displays distributions of aspect values across the study area using GRASS module d.polar by following command: 'd.polar aspect undef=0' with 'undef=0' flag indicating that 'no data' areas are distinct from flat areas where aspect is undefined. The vector lines and length in the polar diagram indicate the direction in the histogram of aspect data.

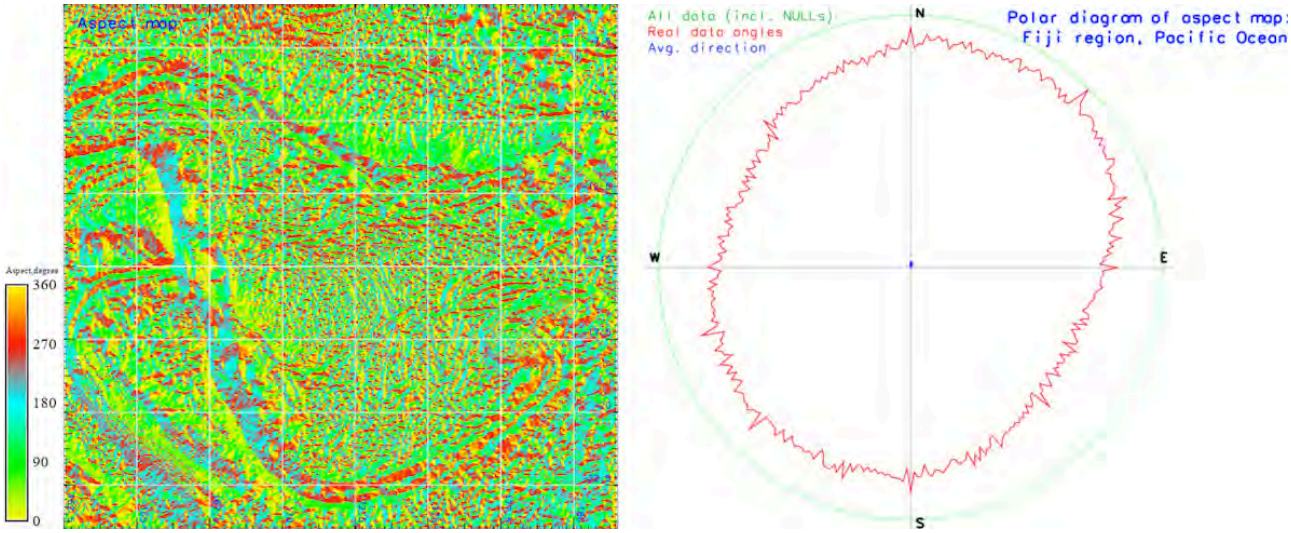

Fig. 6. Topographic analysis of the study area: slope aspect (North-South-West-East disposition of slopes) and its polar diagram showing distribution of the relief values in the region of North Fiji Basin, south Pacific Ocean. Mapping and plotting: GRASS GIS. Source: author.

The concept of the topographic curvature [Fig. 7] is based on the principle of the slope geometry and represents the 2nd derivative of a surface calculated as a parallel to the direction of the maximal slope on a topographic map. Negative curvature value indicate elevations (seamounts on the oceanic floor and mountains and positive relief forms on the land areas), which point that the relief is upwardly convex at that cell in a raster. On the contrary, positive curvature values indicate that the surface is a concave at a raster cell indicating oceanic trench and troughs as well as hollows on the land surface. Thus, curvature of the raster correlates with elevation map [Fig. 7, left] and approximately outline the topographic structures in Fiji area, since these areas have substantial correlation between curvatures and terrain surface relief. Hence, curvature parameter measures rate of the change (positive and or negative variations) in elevation against zero values (gradient) as can be compared with the elevation map [Fig. 7, left and right].

Two histograms [Fig. 8] reveal primary elevation and gravity data groupings: relief of the continents and the oceanic bathymetry (trenches, abyssal plains, shelf areas), roughly between -5,000 and -1,000 meters below sea level, and a clear peak with major values between 100 and 350 m above sea level (land area). This distribution indicates that the area of the dominating values of the ocean floor in North Fiji Basin are between -1,500 to -3,000 m, which has been visualized on Fig. 1 and Fig. 2. The dramatic steepening of the gravity values on the histogram [Fig. 8, right] at values between 50 and 55 mGal and 58 to 63 mGal indicates the geoid undulations which refer to the shape of the ocean surface under the influence of the Earth's gravity without other

factors (winds and tides).

Topographic relief is sensitive to the geological development of the study area and geophysical settings. Tectonic settings formed as a result of plate subduction and slab movements are the most important limiting factor for the submarine bathymetry ultimately affecting the surface of the present relief. Advanced tools of geospatial data analysis, such as GRASS GIS, promotes the development of the new methods and approaches in geological and bathymetric mapping through comparative analysis and overlay of various raster layers, and increases the precision of models.

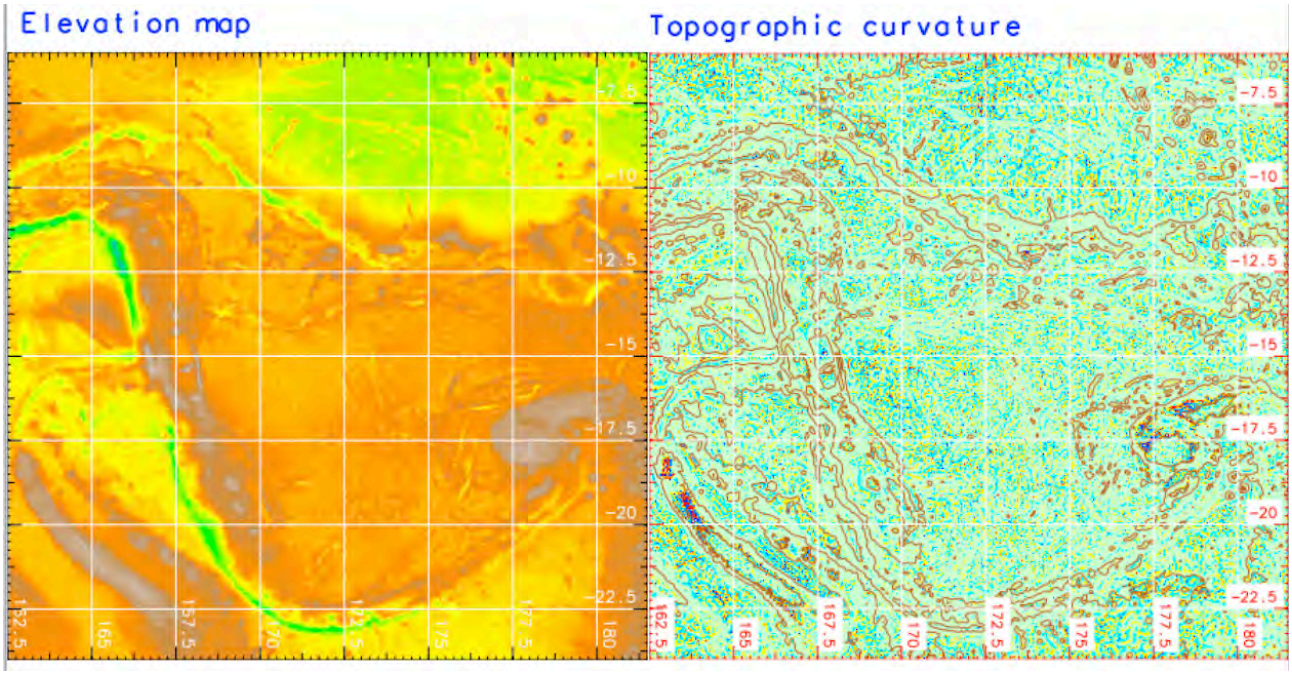

Fig. 7. Relief elevations (left) and topographic curvature (right) in North Fiji Basin, south Pacific Ocean. Mapping: GRASS GIS 7.6. Source: author.

4. Conclusion

Producing a topographic analysis from raster DEMs and mapping geological and geophysical data through a GIS based data analysis is a processes including many steps of geodata analysis. A number of approaches, statistical techniques, algorithms and methodologies have become standard practice in GIS (*Klaučo et al., 2013a, 2013b, 2014, 2017*) and contributed to the data automatization in cartography (e.g. Schenke & Lemenkova, 2008; Gauger et al., 2007; Lemenkova, 2020a, 2020b; *Suetova et al., 2005*). To facilitate this combinatorial experimentation, the paper presented study based on the organized and visualized data on geophysical and geological settings in the unique region of Fiji Basin located in Pacific Ocean, performed by GRASS in a comprehensive, modular framework.

Tested GRASS GIS functionality include a series of modules (r.slope.aspect, r.in.gdal, d.rast, d.vect, g.region, d.polar, d.histogram, d.grid, d.legend, d.text.) which enabled to perform plotting of the topographic maps and visualized geophysical variations along changing the submarine relief of the selected area of Fiji basin, Pacific Ocean. Correlation between the marine free-air gravity anomalies with topographic maps identify subsurface bodies and anomalies within the Earth that are reflected in the topographic shape forms, since density changes of rock bodies have their effect on the acceleration of gravity which can be seen on the maps.

Functionality of the GRASS GIS demonstrated in this research proved it to be an excellent geoinformation system that can process, manage, analyze and display raster and vector data for spatial and attribute topographic analysis. The advantages of GRASS GIS system consist in its module-based structure and ability

to manipulate with multi-source various types of data. Using comparative analysis enables to draw conclusions over bathymetric and geophysical correlations through the analysis of data presented in different monitors (d.mon wx0, d.mon wx1, etc) or as facetted layers. GRASS GIS differ from traditional GIS due to its both console-based and GUI-based approaches.

The development of new methodologies to address the growing new directions in cartography will build upon and extend these standard practices of raster and vector data analysis, requiring experimentation with and recombination of statistical techniques specifically in geography (*Lemenkova, 2019g, 2019h, 2019i, 2019j*). In addition to the existing examples of cross-section profile digitizing my means of Generic Mapping Tools (Lemenkova, 2019a, 2019b, 2019c, 2019d, 2019e, 2019f), the implementation of this data analysis provided an extensible, well-tested toolbox by means of GRASS GIS. In contrast with GMT, GRASS GIS supports both console-based cartographic scripting and Graphical User Interface (GUI) which facilitates mapping.

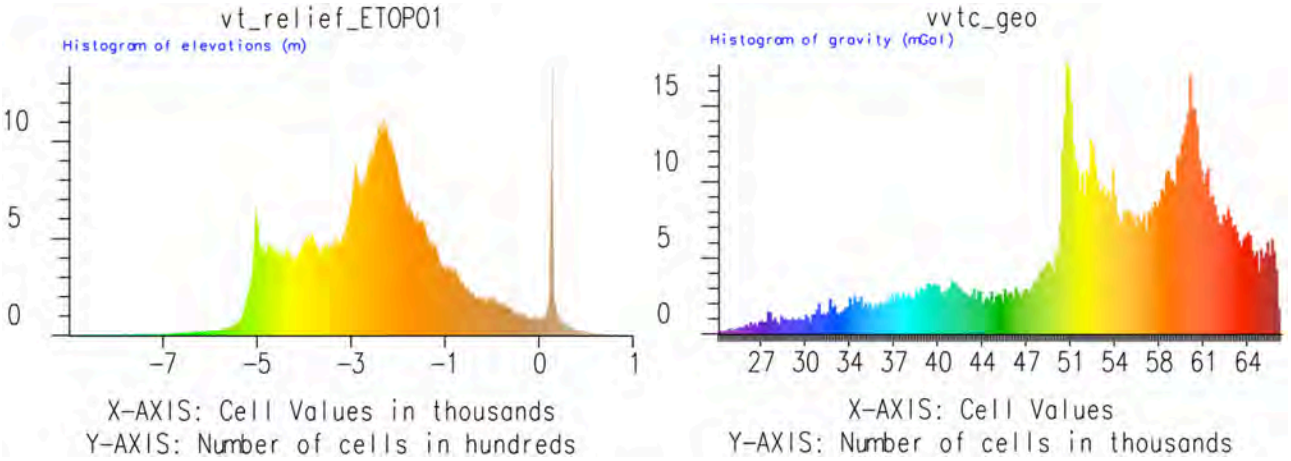

Fig. 8. Histogram of the topographic data distribution (left) and gravimetric values derived from geoid model (right), Fiji region, south Pacific Ocean. Plotting: GRASS GIS 7.6. Source: author.

Since the specifics of GRASS GIS consists in its console-based scripting approach beside a GUI, using GRASS GIS becomes a convenient tool for advanced users of programming languages. Throughout the development of programming, its has become possible to build a framework of the multi-disciplinary data analysis combining both statistical data analysis and GIS visualization that is flexible and extensible (e.g. Lemenkova, *2019l, 2019m, 2019n)*. The toolbox of such integrative approaches includes scripting utilities with spatial data processing, for example, visualization correlation between geological, topographic and geophysical settings, and factor analysis (Lemenkova, *2018a, 2018b*) through numerical data modelling.

Advantages of such approaches consist in the fact that when combining coding for tabular data processing (.csv) with multiple GIS functions are available to help test and verify results of the data derived from GIS including: (a) checking variables attributes for coordinates to visualized data distribution (b) comparing datasets with each other (e.g. geologic values with geomorphological data, slope steepness) as spatial analysis.

These testings can be performed as batch data processing in an a sequential stepwise algorithms (e.g. Lemenkova, *2019k*) and then rapidly transferred and incorporated as template for other study area (for example testing different trenches across the Pacific Ocean and going beyond to other areas: Atlantic Ocean, Indian Ocean), to ensure that variations in spatial applications do not change the principal functionality of the data model. The presented GRASS GIS approach for topographic analysis and mapping is a contribution to the development and application of cartographic tools for geophysical mapping and spatial analysis.

Acknowledgment

"This research was implemented in the framework of the project No. 0144-2019-0011, Schmidt Institute of Physics of the Earth, Russian Academy of Sciences and China Scholarship Council (CSC), State Oceanic Administration (SOA), Marine Scholarship of China, Grant Nr. 2016SOA002, People's Republic of China."

References

[1] ANDERSEN, O.B., KNUDSEN, P., BERRY, P.A.M., (2009), *The DNSC- 08GRA global marine gravity field from double retracked satellite altimetry*, Journal of Geodesy, 84(3), 191–199

[2] AUZENDE, J.M., LAGABRIELLE, Y., SCHAAF, A., GENTE, P.,AND EISSEN, J.P., (1986), *Tectonique intra-océanique décrochante à l'ouest des îles Fidji (Bassin Nord Fidjien)*. Campagne SEAPSO III du N. O. Jean Charcot, C. R. Acad. Sci. Paris, 303:241-246

[3] AUZENDE, J.-M., PELLETIER, B., EISSEN, J.-P., (1995), *The North Fiji Basin geology, structure, and geodynamic evolution*, Backarc Basins. Springer. 139–175

[4] BENDEL, V., (1993), *Cadre géologique et composition des minéralisations hydrothermales en contexte arrière-arc: exemple de la dorsale du Bassin Nord Fidjien*, Thèse Université Brest, France

[5] BOESPFLUG, X., (1990), *Evolution géodynamique et géochimique des bassins arrière-arcs. Exemples des bassins d'Okinawa, de Lau et Nord-Fidjien*, Thèse, Université Brest, France

[6] COLLOT, J.Y., DANIEL, J., BURNE, R.V., (1985), *Recent tectonics associated with the subduction/ collision of the d'Entrecasteaux Zone in the central New Hebrides*, Tectonophysics 11, 325–356

[7] CRAWFORD, W.C., HILDEBRAND, J.A., DORMAN, L.M., WEBB, S.C., WIENS, D.A., (2003), *Tonga Ridge and Lau Basin Crustal Structure from Seismic Refraction Data*, Journal of Geophysical Research: Solid Earth, 108 (4): 2195

[8] DANIEL, J., (1982), *Morphologie et structures superficielles de la partie sud de la zone de subduction des Nouvelles-Hébrides, in Contribution à l'étude géodynamique du Sud-Ouest Pacifique, Equipe de Géologie-Géophysique du Centre ORSTOM de Nouméa,* Travaux et Documents de I'ORSTOM 147:39-60

[9] DAVEY, F.J., (1982), *The structure of the South Fiji Basin*, Tectonophysics 87, 185–241

[10] DUBOIS, J., PASCAL, G., BARAZANGI, M., ISACKS, B. L., AND OLIVER, J., (1973), *Travel times of seismic waves between the New Hebrides and Fiji Islands: A zone of low velocity beneath the Fiji Plateau*, Journal of Geophysical Research, 783431-3436

[11] FISHER, R.L., HESS, H.H., HILL, M.N., (1963), *Trenches*. The Sea v. 3 The Earth Beneath the Sea. New York: Wiley-Interscience, 411–436

[12] GARCIA, E., SMITH, W.H.F., SANDWELL, D.T., (2013), *Retracking CryoSat-2, Envisat, and Jason-1 radar altimetry waveforms for improved gravity field recovery*, Revised for Geophysics Journal International, June 2013

[13] GRACIA-MONT, E., (1991), *Etude morphostucturale du segment N 160" la dorsale du Basin Nord-Fidjien, Analyse des donnees de la campagne Yokosuka 90*, Rapport de D.E.A., Universite de Bretagne Occidentale, Brest

[14] GAUGER, S., KUHN, G., GOHL, K., FEIGL, T., LEMENKOVA, P., HILLENBRAND, C., (2007), *Swath-bathymetric mapping*, Reports on Polar and Marine Research, 557, 38–45

[15] GAYNANOV A.G., (1980), *Gravimetric studies of the Earth's crust of the oceans*, Moscow: Moscow State University Press, 240 pp

[16] GILL, J. B., (1976), *Composition and Age of Lau Basin and Ridge Volcanic Rocks: Implications for Evolution of an Interarc Basin and Remnant Arc,* Bulletin of the Geological Society of America 87(10): 1384–1395

[17] HAHM, D., HILTON, D.R., CASTILLO, P.R., HAWKINS, J.W., HILTON, D.R., HANAN, B.B., HAURI, E.H., (2012), *An overview of volatile systematics of the Lau Basin — resolving the effects of source variation, magmatic degassing and crustal contamination*, Geochimica et Cosmochimica Acta, 85, 88–113

[18] HAWKINS, J.W., BLOOMER, S.H., EVANS, C.A., MELCHIOR, J.T., (1984), *Evolution of Intra-Oceanic Arc-Trench Systems*, Tectonophysics, 102 (1–4): 175–205

[19] HESS, H.H., (1962), *History of ocean basins*, In: Engel, A.E.J., James, H.L., Leonard, B.F. (Eds.), Petrologic Studies: A Volume in Honor of A.F. Buddington. Geological Society of America,

Boulder, CO, 599–620

[20] HOFIERKA, J., MITASOVA, H., NETELER, M., (2009), *Terrain parameterization in GRASS*. In T. Hengl and H.I. Reuter, editors, Geomorphometry: concepts, software, applications

[21] ISHIBASHI, J.I., WAKITA, H., NOJIRI, Y., GRIMAUD, D., JEAN-BAPTISTE, P., GAMO, T., AUZENDE, J.M., URABE, T., (1994), *Helium and carbon geochemistry of hydrothermal fluids from the North Fiji Basin spreading ridge (southwest Pacific)*, Earth and Planetary Science Letters 128, 183–197

[22] KELLER, N., ARCULUS, R.J., HERMANN, J., RICHARDS, S., (2007), *Submarine back-arc lava with arc signature: Fonualei spreading centre, northeast Lau basin, Tonga*, Journal of Geophysical Research, 113, B08S07

[23] KIOUS, W.J., TILLING, R.I., (1996), *This Dynamic Earth: The Story of Plate Tectonics*, U.S. Government Printing Office, Washington, DC

[24] KLAUČO, M., GREGOROVÁ, B., STANKOV, U., MARKOVIĆ, V., LEMENKOVA, P., (2013a), *Determination of ecological significance based on geostatistical assessment: a case study from the Slovak Natura 2000 protected area*, Central European Journal of Geosciences, 5(1), 28-42

[25] KLAUČO, M., GREGOROVÁ, B., STANKOV, U., MARKOVIĆ, V., LEMENKOVA, P., (2013b), *Interpretation of Landscape Values, Typology and Quality Using Methods of Spatial Metrics for Ecological Planning,* in: 54th International Conference Environmental & Climate Technologies (Riga Technical University, Oct. 14, 2013). Riga, Latvia

[26] KLAUČO, M., GREGOROVÁ, B., STANKOV, U., MARKOVIĆ, V., LEMENKOVA, P., (2014), *Landscape metrics as indicator for ecological significance: assessment of Sitno Natura 2000 sites, Slovakia, Ecology and Environmental Protection*, Proceedings of the International Conference (Belarusian State University, March 19–20, 2014). Minsk, Belarus, 85–90

[27] KLAUČO, M., GREGOROVÁ, B., STANKOV, U., MARKOVIĆ, V., LEMENKOVA, P., (2017), *Land planning as a support for sustainable development based on tourism: A case study of Slovak Rural Region*, Environmental Engineering and Management Journal, 2(16), 449–458

[28] LEMENKOVA, P., (2019a), *Automatic Data Processing for Visualising Yap and Palau Trenches by Generic Mapping Tools*, Cartographic Letters, 27 (2), 72–89

[29] LEMENKOVA, P., (2019b), *Geomorphological modelling and mapping of the Peru-Chile Trench by GMT*, Polish Cartographical Review, 51 (4), 181–194

[30] LEMENKOVA, P., (2019c), *Plotting Ternary Diagrams by R Library ggtern for Geological Modelling*, Eastern Anatolian Journal of Science, 5 (2), 16–25

[31] LEMENKOVA, P., (2019d), *Geophysical Modelling of the Middle America Trench using GMT*, Annals of Valahia University of Targoviste, Geographical Series, 19(2), 73–94

[32] LEMENKOVA, P., (2019e), *Topographic surface modelling using raster grid datasets by GMT: example of the Kuril-Kamchatka Trench, Pacific Ocean*, Reports on Geodesy and Geoinformatics, 108, 9–22

[33] LEMENKOVA, P., (2019f) GMT Based Comparative Analysis and Geomorphological Mapping of the Kermadec and Tonga Trenches, Southwest Pacific Ocean, Geographia Technica, 14(2), 39–48

[34] LEMENKOVA, P., (2019g), *Testing Linear Regressions by StatsModel Library of Python for Oceanological Data Interpretation*, Aquatic Sciences and Engineering, 34, 51–60

[35] LEMENKOVA, P., (2019h), *Regression Models by Gretl and R Statistical Packages for Data Analysis in Marine Geology*, International Journal of Environmental Trends, 3(1), 39–59

[36] LEMENKOVA, P., (2019i), *Numerical Data Modelling and Classification in Marine Geology by the SPSS Statistics*, International Journal of Engineering Technologies, 5(2), 90–99

[37] LEMENKOVA, P., (2019j), *Geospatial Analysis by Python and R: Geomorphology of the Philippine Trench, Pacific Ocean,* Electronic Letters on Science and Engineering, 15 (3), 81–94

[38] LEMENKOVA, P., (2019k), *AWK and GNU Octave Programming Languages Integrated with Generic Mapping Tools for Geomorphological Analysis*, GeoScience Engineering, 65 (4), 1–22

[39] LEMENKOVA, P., (2019l), *Statistical Analysis of the Mariana Trench Geomorphology Using R Programming Language*, Geodesy and Cartography, 45(2), 57–84

[40] LEMENKOVA, P., (2019m), *An Empirical Study of R Applications for Data Analysis in Marine Geology*, Marine Science and Technology Bulletin, 8(1), 1-9

[41] LEMENKOVA, P., (2019n), *Processing oceanographic data by Python libraries NumPy,*

SciPy and Pandas, Aquatic Research, 2, 73-91

[42] LEMENKOVA, P., (2020a), *Visualization of the geophysical settings in the Philippine Sea margins by means of GMT and ISC data*, Central European Journal of Geography and Sustainable Development, 2(1), 5–15

[43] LEMENKOVA, P., (2020b), *GMT-based geological mapping and assessment of the bathymetric variations of the Kuril-Kamchatka Trench, Pacific Ocean*, Natural and Engineering Sciences, 5(1), 1–17

[44] LEMENKOVA, P., (2018a), *R scripting libraries for comparative analysis of the correlation methods to identify factors affecting Mariana Trench formation*, Journal of Marine Technology and Environment, 2, 35–42

[45] LEMENKOVA, P., (2018b), *Factor Analysis by R Programming to Assess Variability Among Environmental Determinants of the Mariana Trench*, Turkish Journal of Maritime and Marine Sciences, 4, 146–155

[46] LITVIN, V.M., (1987), *Morphostructure of the ocean floor*, Nedra, 311 p

[47] MAILLET, P., EISSEN, J.P., LAPOUILLE, A., MONZIER, M., BALEIVANUALALA, V., BUTSCHER, J., GALLOIS, F., LARDY, M., (1986), *La dorsale active du bassin Nord-Fidjien entre 20's et 20"53'S: Signature magnétique et morphologique*, C.R. Acad. Sci. Paris 302(II):135-140

[48] MAILLET, P., MONZIER M., EISSEN, J.P., LOUAT R., (1989), *Geodynamics of an arc ridge junction: The case of the New Hebrides arc-North Fiji Basin*, Tectonophysics, 165: 251-268

[49] NETELER, M., (2000), *GRASS-Handbuch*, Geosynthesis 11. University of Hannover. Der praktische Leitfaden zum Geographischen Informationssystem GRASS

[50] NETELER, M., MITASOVA, H., (2008), *Open Source GIS. A GRASS GIS Approach*, 3rd Edition. ISBN-13: 978-0- 387-35767-6 NY: Springer, 417 p

[51] SANDWELL, D.T., SMITH, W.H.F., (2009), Global marine gravity from retracked Geosat and ERS-1 altimetry: Ridge segmentation versus spreading rate: Journal of Geophysical Research, 114, no. B1, B01411, B0141

[52] Sandwell, D.T., Smith, W.H.F. (2005), *Retracking ERS-1 altimeter waveforms for optimal gravity field recovery*, Geophysical Journal International, 163, no. 1, 79–89

[53] SCHENKE, H. W., LEMENKOVA, P., (2008), *Zur Frage der Meeresboden-Kartographie: Die Nutzung von AutoTrace Digitizer für die Vektorisierung der Bathymetrischen Daten in der Petschora-See*, Hydrographische Nachrichten, 81, 16–21

[54] SUETOVA, I. A., USHAKOVA, L. A., LEMENKOVA, P., (2005), *Geoinformation mapping of the Barents and Pechora Seas*, Geography and Natural Resources, 4, 138–142

[55] TAYLOR, B., ZELLMER, K., MARTINEZ, F., GOODLIFFE, A., (1996), *Sea-floor Spreading in the Lau Back-arc Basin*, Earth and Planetary Science Letters. 144 (1–2): 35–40WINGHAM, D., FRANCIS, C. R., BAKER, S., BOUZINAC, C., BROCKLEY, D., CULLEN, R., DE CHATEAU-THIERRY, P., LAXON, S. W., MALLOW, U., MA- VROCORDATOS, C., PHALIPPOU, L., RATIER, G., REY, L., ROSTAN, F., VIAU, P., AND WALLIS, D. W., (2006), *CryoSat-2: A mission to determine the fluctuations in Earth's land and marine ice fields*, Advances in Space Research, 37(4), 841–871